Chapter 18

Models of Refractive Error Development

George K. Hung[1] and Kenneth J. Ciuffreda[2]

[1]*Dept. of Biomedical Engineering, Rutgers University, 617 Bowser Rd., Piscataway, NJ 08854-8014, PH: (732) 445-4137, FX: (732) 445-3753, EM: shoane@rci.rutgers.edu;*

[2]*Dept. of Vision Sciences, State University of New York, State College of Optometry, 33 West 42nd St., New York, NY 10036; PH: (212) 780-5132, FX: (212) 780-5124; EM: kciuffreda@sunyopt.edu.*

18.1 INTRODUCTION

Clarity of the visual image is a vital component of ocular health. A common method for assessing image clarity is to measure distance visual acuity. The development of an uncorrected refractive error, however, reduces visual acuity, and in turn adversely impacts upon the quality of ocular health. This chapter discusses various analytical approaches taken in the understanding of refractive error development.

There are two main types of refractive error: hyperopia and myopia. Hyperopia, or farsightedness, occurs when the combined optical power of the cornea and the unaccommodated lens are less than that needed for the axial length of the eye, so that the retinal image is focused beyond the retina. On the other hand, myopia, or nearsightedness, occurs when the total ocular power of the eye exceeds that needed for its ocular length, so that the image is focused in front of the retina. Image clarity for the distant object in hyperopes can be attained by means of accommodation, or an increase in lens power, but at the expense of increased effort along with a reduced effective accommodative range. For myopes, however, image clarity cannot be attained with increased accommodation, and in fact, this would further degrade retinal-image clarity. Thus, myopia is associated with the more immediate concerns of everyday visual function.

Myopia is a worldwide public health concern (Goldschmidt, 1968), because it affects 25% of the adult population in the United States (Sperduto et al, 1983) and 75% or more of the adult population in Asian countries such as Taiwan (Lin et al, 1996). It can be corrected by optical means, but the estimated annualized cost to consumers in the United States for eye examinations and corrective lenses is $4.6 billion (Javitt and Chiang, 1994). Furthermore, the wearing of spectacles for myopia may restrict one's vocational and avocational options (Mahlman, 1982). Surgical techniques to reduce myopia are available, but they are expensive (Grosvenor and Goss, 1999). Furthermore, despite the continual developments and technological improvements over the past 20 years, there are still surgical and post-surgical risks, along with possible side effects such as long-term hazy vision (Javitt and Chiang, 1994). Moreover, surgery does not prevent the subsequent development of adult-onset myopia or other age-related refractive changes, for example, due to increased lens index and presbyopia (Javitt and Chiang, 1994). For these reasons, the slowing of myopic progression, as well as the prevention of its initial occurrence, has been of considerable interest to clinicians and scientists alike for decades.

To understand the fundamental mechanisms underlying refractive error development, both *genetic* and *environmental* factors must be examined (Ong & Ciuffreda, 1997; McBrien & Millodot, 1986; Gwiazda et al, 1993; Mutti et al, 1996; Jiang & Woessner, 1996; Grosvenor and Goss, 1999). Evidence for genetic influence is evident in the high correlation between refractive errors in twins (Kimura, 1965; Sorsby et al, 1962; Goss et al, 1988), and the higher prevalence of myopia in children whose parents were also myopic (Gwiazda et al, 1993). On the other hand, evidence for environmental influence comes from the very rapid increase in the prevalence of myopia in the Intuit, Japanese, Chinese, and Native Americans over the past 50 years (Young et al, 1969; Alward et al, 1985; Hosaka, 1988; Goh and Lam, 1994; and Lam et al, 1994; Woodruff and Samek, 1977), suggesting an association between their progressively greater amount of time spent on nearwork during formal schooling and higher rates of childhood myopia prevalence and progression (Pãssinen et al, 1989; Wu et al, 1999; Zhang et al, 2000). Clearly, both genetic and environmental factors are involved.

During infancy under normal genetic development, there is an inherent mismatch between the optical power of the cornea/lens and the axial length of the eyeball (Scammon & Armstrong, 1925). Yet, as the normal eye matures, the cornea/lens and ocular tunics begin to develop in concert to provide a relatively precisely focused image on the retina (Bennett & Rabbetts, 1989; Grosvenor and Goss, 1999). This process is called emmetropization (Yackle & Fitzgerald, 1999). Clearly, certain critical information is used to coordinate cornea/lens and axial growth. One of the

most important cues for regulating axial growth appears to be retinal-image defocus (McBrien & Millodot, 1986; Ong & Ciuffreda, 1997; Wallman, 1997; Norton, 1999), which is dependent on the interaction of both cornea/lens and axial length. Cornea/lens growth and its consequent change in optical power will alter retinal-image defocus, but an appropriate change in the axial length growth rate will act to reduce this defocus, and in turn restore the balance between these two components. Since the basic growth of the cornea/lens is genetically-predetermined (Sorsby et al, 1962; Goss and Erickson, 1987; Goss and Jackson, 1993; Fledelius and Stubgaard, 1986), emmetropization involves only the regulation and modulation of axial length growth (McBrien and Millodot, 1986; Ong and Ciuffreda, 1997; Wallman, 1997; Norton, 1999).

Emmetropization also occurs under environmentally-induced conditions. This is seen in numerous studies which have attempted to determine the effect of various optically-based manipulations of retinal-image quality on induced ocular growth and refractive development. The findings have been mixed with respect to the resultant direction of refractive shift. Some manipulations produced a myopic shift. These included: prolonged nearwork (Goss and Wickham, 1993; Grosvenor & Goss, 1999), purposeful undercorrection for myopia (O'Leary, 2000), graded diffusers (Smith and Hung 2000), and black occluder contact lenses (Tigges et al, 1990; Iuvone et al, 1991). On the other hand, other manipulations resulted in a hyperopic shift. These included: very strong diffusers (O'Leary et al, 1992; Bradley et al, 1996), crystalline lens removal (Wilson et al, 1987), and initial imposition of graded diffusers (Smith & Hung, 2000). Finally, manipulations using plus or minus lenses in the chick (Schaeffel et al, 1990), tree shrew (Norton, 1999; Siegwart & Norton, 1999), and monkey (Smith & Hung, 1999) resulted in either hyperopic or myopic growth, respectively.

Thus, emmetropization occurs during both normal genetically-determined ocular growth and under environmentally-induced conditions, and it involves the regulation of axial length growth rate via some property of retinal-image defocus. It appears to be effective following temporary optical manipulations, such as that seen for imposed plus and minus lenses, in which the eye responds by changing its axial length growth rate appropriately to compensate for the optical defocus. However, it has been thought that with prolonged nearwork, emmetropization breaks down, so that the axial length continues to increase, thus resulting in the development of myopia.

The mechanism for the short-term emmetropization process appears to be relatively simple, since visual feedback related to retinal-image defocus could provide the requisite control signal to regulate the direction and magnitude of axial growth. However, such appropriate changes in growth rate occur even when the optic nerve is severed (Troilo et al, 1987; Wildsoet & Pettigrew, 1988) or the midbrain nuclei for controlling accommodation are lesioned (Troilo, 1989), thus precluding any central visual feedback

mechanism. Moreover, since defocus blur per se is an even-error signal (Stark, 1968), it lacks the requisite directional sensitivity for controlling axial growth. For these reasons, the controlling mechanism for the short-term emmetropization process, and in turn the long-term development of myopia, has remained a puzzle for decades.

18.2 EARLIER MODELS

Various descriptive as well as quantitative models have been proposed to account for the emmetropization process and the development of refractive error (Medina, 1987; Medina and Fariza, 1993; Schaeffel & Howland, 1988; Bartmann & Schaeffel, 1994; Flitcroft, 1998; Blackie & Howland, 1999; Hung & Ciuffreda, 1999; Norton, 1999; Wick, 2000). However, these models have not been able to explain the fundamental underlying mechanism of refractive error development.

For example, Medina and Fariza model (Fig. 18.1a) proposed a model whose simulated output curve matched the experimental refractive error development timecourse. Thus, the time constant, k, was selected to be very large (about 10 years) to fit the refractive error vs. age curve (see Fig. 18.1b). However, the model lacked homeomorphic correspondence with physiological processes associated with refractive error development and emmetropization. And, as such, the model simply served as a curve fitting mechanism, but would not be able to respond to stimulus changes such as those employed in the experimental optical manipulations discussed above.

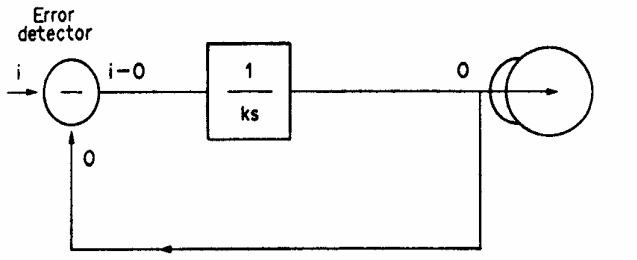

Figure 18.1(a). Servo mechanism of emmetropization proposed by Medina and Fariza (1993). The refractive error is controlled by a feedback system: i, input or commanded refraction; o, output or measured refraction; i - o, error. Transfer function F(s) = O(s) / I(s) = 1 / (1+ks) is of first-order in s, where s is a complex variable, k is the time constant, and O(s) and I(s) are the Laplace transforms of the temporal input and output function. Reprinted from Medina and Fariza (1993), pg.23, Fig. 1, with permission of Elsevier Science.

Figure 18.1(b). Refractive error vs age plot for experimental data (square symbols) and model (solid curve). Note that the time constant (estimated as the time to reach a change in exponential response that is 63% of the final difference in amplitude) for the curve is about 10 years. Reprinted from Medina and Fariza (1993), pg. 25, Fig. 3, with permission of Elsevier Science.

Schaeffel and Howland (1988) proposed a model in which two independent feedback loops were assumed to regulate ocular growth (Fig. 18.2). The accommodative loop operated under crystalline lens optical power feedback, whereas the retinal loop operated under local retinal feedback without accommodation. They presented simulation results showing that the accommodative feedback loop (Fig. 18.2, left loop) was responsible for the imposed-lens experimental results and also for the transient hyperopia observed after sectioning the optic nerve and lesioning the Edinger-Westphal nucleus. On the other hand, the retinal feedback loop (Fig. 18.2, right loop) was responsible for form-deprivation myopia, myopia in restricted retinal areas, myopia after optic nerve section, and recovery from form-deprivation myopia even with lesioning of the Edinger-Westphal nucleus. However, the model did not provide for interaction between accommodation and retinal feedback, which would have been expected to occur normally (Ciuffreda, 1991; 1998; also see Chapter 8, Models of Accommodation, in this volume). In addition, they had to vary the gains of both loops to simulate the experimental results. Yet, such gain variations should not have been permitted except in unusual cases, such as the simulation of an adaptive control system (Hung, 1992). Moreover, the increased degrees of freedom provided by gain adjustments in the two feedback loops may have resulted in an artificial, and not physiologically justified, matching of model and experimental data.

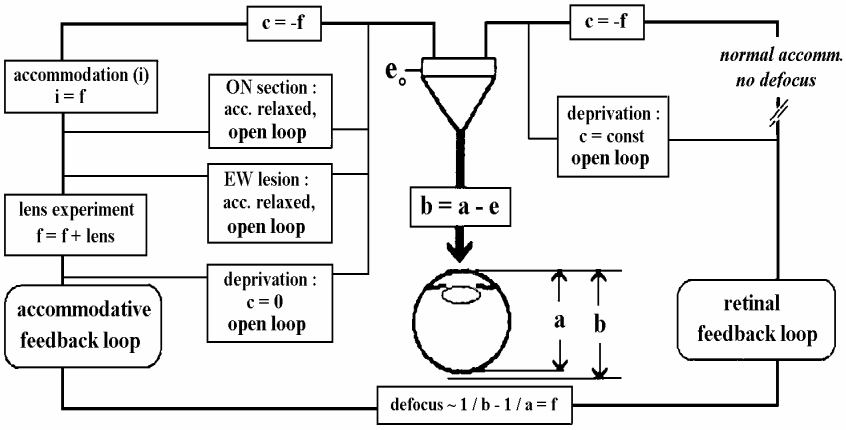

Figure 18.2. Model of refractive error development proposed by Schaeffel and Howland (1988) consists of independent accommodative and retinal feedback loops that regulate ocular growth. Symbols: a = control or reference axial length of the eye, b = current axial length, c = correction signal derived from either accommodative or retinal feedback, e_0 = initial difference between control and current axial length, EW = Edinger-Westphal nucleus, f = refractive state of the eye, lens = imposed lens optical power, ON section = optic nerve section, i = average amount of accommodation due to hyperopic defocus. Reprinted from Schaeffel and Howland (1988), pg. 2083, Fig. 2, with permission of Optical Society of America.

Flitcroft (1998) proposed a model of emmetropization and myopia (Fig. 18.3) using the dual-interactive accommodation and vergence feedback model by Hung and colleagues (1990, 1992, 1996, 1997). Refraction was defined as a function of the integral of the accommodative error, or blur, which could be obtained via solution of the accommodative and vergence interactive feedback equations (Hung, 1990). Simulations of the model using various initial refractions and a selected set of interactive accommodation-vergence model parameter values based on Hung (1996) was believed to demonstrate emmetropization of the response towards a constant refraction level (Fig. 18.3b). Analysis of the model, however, revealed that it simply generated decay curves that asymptote to a specified level rather than being an actual dynamic emmetropization mechanism that compensated for the imposed retinal defocus.

Flitcroft's (1998) model is based on the equation

$$r_{t+1} = r_t - k \int a_{error}(t)dt \tag{18.1}$$

with

$$a_{error} = ae + r \tag{18.2}$$

where r is refractive correction, t is time, k is gain of the emmetropization process, ae is accommodative error (or accommodative stimulus minus accommodative response), and a_{error} is net accommodative error. The accommodative error was obtained by the solution of the static interactive accommodative and vergence model equations provided by Hung (1996) and organized in a slightly different form by Flitcroft (1998). For simplicity in analyzing Eq. 18.1 without a loss of generality, the depth of focus was not included. For this analysis, time domain variables will be designated by lower case, whereas the Laplace transform variables will be designated by upper case. One can rewrite Eq. 18.1 as

$$dr = -k \int (ae + r)\, dt \tag{18.3}$$

Taking the derivative of both sides of Eq. 18. 3 gives

$$\frac{dr}{dt} = -k \bullet (ae + r) \tag{18.4}$$

Taking the Laplace transform of both sides of Eq. 18.4 gives

$$s \bullet R - r(0^+) = - k\,(AE + R) \tag{18.5}$$

where s is the Laplace operator, and $r(0^+)$ equals the initial value of refraction, with the + symbol designating the value immediately after time 0. Let AE = ae/s, which represents a unit step of accommodative error. Re-arranging and solving for R gives

$$R = - k \bullet ae \bullet \frac{1}{s + k} \bullet \frac{1}{s} \; + \; \frac{r(0^+)}{s + k} \tag{18.6}$$

Taking the partial fraction expansion of the product term in Eq. 18.6 gives

$$R = ae \bullet \left(\frac{1}{s+k} - \frac{1}{s} \right) + \frac{r(0^+)}{s+k} \tag{18.7}$$

Taking the inverse transform and re-arranging gives

$$r = \left[r(0^+) + ae \right] \bullet e^{-kt} - ae \tag{18.8}$$

Therefore, the refraction in Flitcroft's model is comprised of the sum of two terms: (1) an exponential decay term whose initial value depends on the initial refraction and the accommodative error, which then decays with a time constant of (1/k) towards a zero value; and (2) a constant bias term given by (-ae) which determines the final steady-state value of the simulation response (see Fig. 18.3b). Hence, instead of being a feedback process that acts on some fundamental property of the retinal-image defocus, the model simply sets the response to eventually arrive at the pre-selected (-ae) level. Moreover, the various initial refractions simply change the initial condition for the prescribed exponential decay of the response curve. Thus, although the model has some of the decay characteristics expected of an emmetropization model, it is clearly not an emmetropization model. Nevertheless, using this model, Flitcroft (1998) developed a relationship between refraction and oculomotor parameters. One of his conclusions based on the simulations was that "an appropriate spectacle correction … imposed after the model has reached a stable myopic refraction due to a high near work demand … has the effect of destabilising the refraction and causing a further myopic shift". On the other hand, recent human experimental results showed greater myopic progression in undercorrected (by approximately 0.75 D) than fully corrected myopic subjects (O'Leary, 2000). Also, animal experimental results (Schaeffel et al, 1990; Siegwart and Norton, 1999; Smith and Hung, 1999) demonstrated myopic growth of the eye with large negative lenses. Thus, both experimental results show myopic progression with large rather than small retinal defocus, which contrasts with Flitcroft's simulation results.

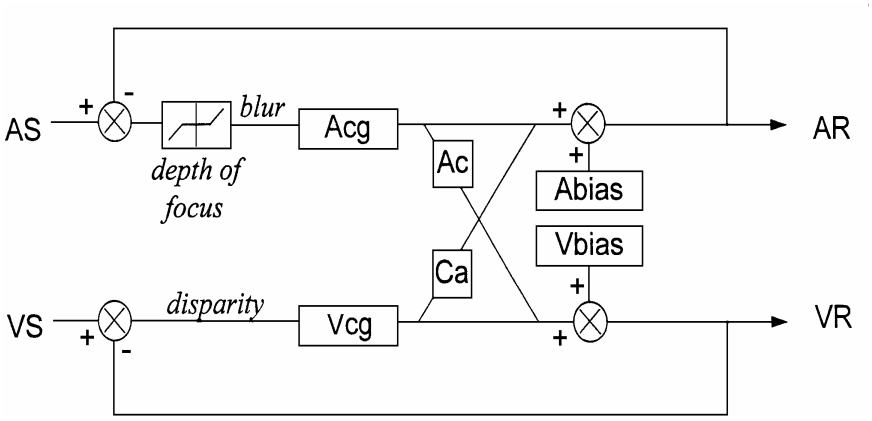

Figure 18.3a. Flitcroft (1998) model of emmetropization and myopia using the dual-interacting feedback model of Hung and colleagues (1980, 1990, 1992, 1996, 1997). AS and VS = accommodative and vergence demand. AR and VR = accommodative and vergence response. ACG and VCG = gains of the accommodative and vergence controllers. ABIAS and VBIAS = tonic level of accommodation and vergence. AC and CA = gain of accommodative convergence and convergence-accommodation crosslink. Reprinted from Flitcroft (1998), pg. 2870, Fig. 1, with permission of Elsevier Science.

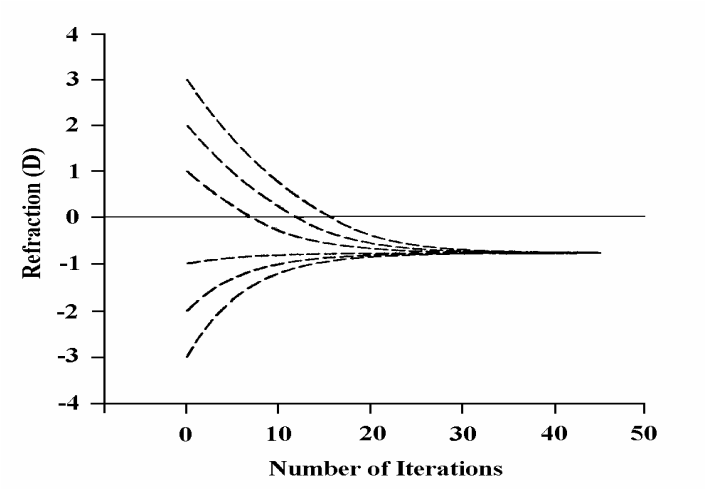

Figure 18.3b. Simulation of Flitcroft (1998) model for refraction as a function of number of interations (in arbitrary time units) for various initial refractions and a selected set of interactive accommodative-vergence model parameter values (based on Hung, 1996) believed to show emmetropization towards a fixed refraction value of about 1 D myopia. Reprinted from Flitcroft (1998), pg. 2874, Fig. 5a, with permission of Elsevier Science.

Hung and Ciuffreda (1999) proposed a descriptive block diagram model of refractive error development (Fig. 18.4a). The main concept of the model is that there are two pathways that interact, which can lead to the development of refractive error. First, a genetically-controlled pathway governs the growth of the cornea, lens, and axial length. A match between the optical and axial length components will result in emmetropia, whereas a mismatch will result in a refractive error. Both normal and abnormal preprogrammed growth are possible. Second, an environmentally-controlled pathway is driven by retinal defocus from the accommodative feedback loop. Subthreshold amounts of retinal defocus do not increase the axial length, whereas prolonged exposure to suprathreshold amounts of retinal defocus will increase the axial length. The genetically-preprogrammed axial length is summed with the environmentally-induced axial length to result in the overall axial length. The difference between cornea/lens optical power and the overall axial length optical power is the refractive error. Any refractive error will in turn serve as a portion of the accommodative stimulus in the accommodative feedback loop.

In addition, a more detailed quantitative version of this model was developed (Hung and Ciuffreda, 1999; Fig. 18.4b). In the basic accommodative (lower) loop, the difference between accommodative stimulus AS and response AR gives the accommodative error AE, which represents retinal defocus. This signal is input to deadspace element (±DSP) representing the depth-of-focus. The output of the deadspace element is input to the accommodative controller, which is represented by a dynamic element with gain ACG and time constant τ_C (= 4 sec). Other components added to the basic loop include a proximal element, an adaptive element, convergence accommodation crosslink gain, tonic accommodation (ABIAS), and lens plant with time constant τ_P (= 0.3 sec). Added to this basic loop is a long-term growth (upper) loop that is driven in part by the root-mean square (rms; equal to the average of the absolute value of the instantaneous response over a given time interval) of the accommodative error (AE), which can contribute to axial growth. Another part of the long-term growth loop is driven by genetic control of the cornea/lens and axial length (τ_E = 9 yrs; τ_F = 2 yrs; and τ_G = 9 years, for late-onset myopes; Hung and Ciuffreda, 1999).. The environmental (i.e., retinal-defocus induced) and genetically-controlled axial lengths are added together to provide the total axial length. Any mismatch between the power for the cornea/lens and the axial length results in a refractive error. Thus, this model provides a basis for both genetically-preprogrammed and environmentally-induced interactive development of refractive error.

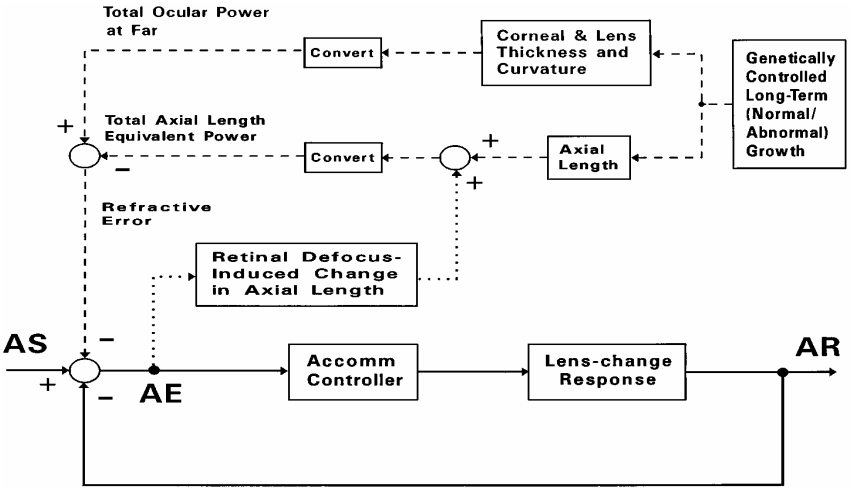

Fig. 18.4a.

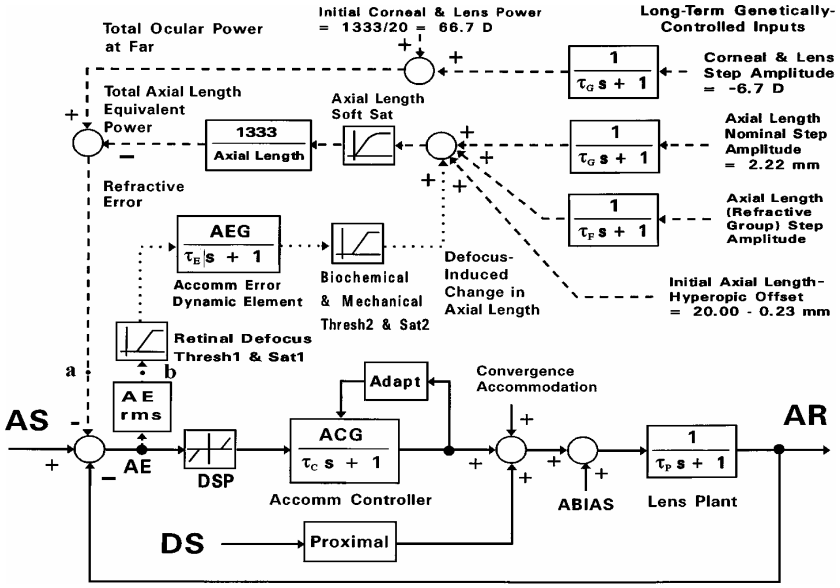

Fig. 18.4b.

Figure 18.4. (a) Descriptive block diagram of refractive error development (Hung and Ciuffreda, 1999). Solid-line pathway represents the normal accommodative system, whereas the dashed-line pathway represents refractive error development derived from both genetically-preprogrammed and retinal-defocus drives to refractive error. (b) Detailed block diagram of refractive error development. Reprinted from Hung and Ciuffreda (1999), pg. 43, Fig. 2A, and pg. 44, Fig. 2B, with permission of Swets and Zeitlinger.

The model was simulated using MATLAB/SIMULINK for the four refractive groups: hyperopes (HYP), emmetropes (EMM), early-onset myopes (EOM), and late-onset myopes (LOM) (Fig. 18.5). The time courses are consistent with experimental data.

Although this model provided important insight into the interactions between genetically-preprogrammed and environmental components, it nevertheless still did not uncover the fundamental underlying mechanism in the development of refractive error.

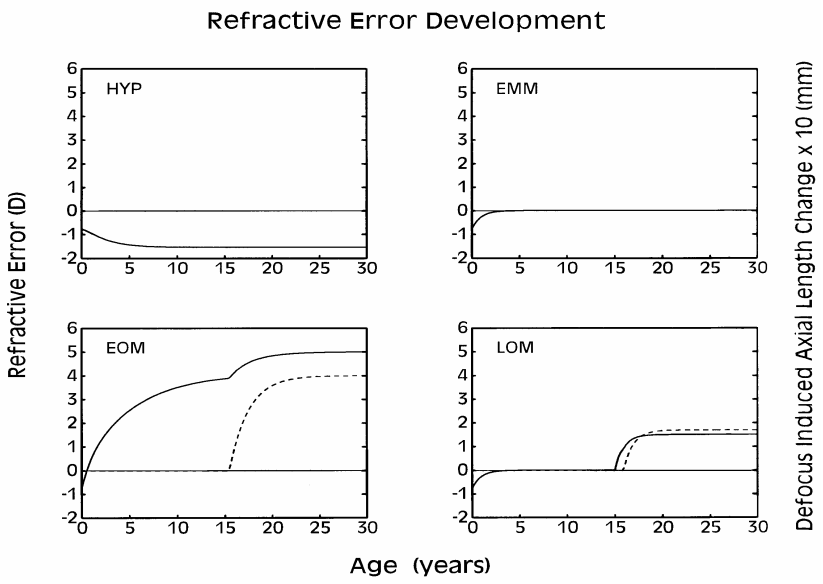

Figure 18.5. Simulation of model using SIMULINK showing long-term (30 yrs) timecourses for refractive error (solid) development and axial length change (dashed) in different refractive groups that are consistent with experimental data. Reprinted from Hung and Ciuffreda (1999), pg. 48, Fig. 5, with permission of Swets and Zeitlinger.

Wick (2000) proposed a conceptual model of emmetropization (Fig. 18.6) and myopia similar to that by Hung and Ciuffreda (1999). However, there are some important differences between the two models. Wick's model provides for separate paths for refractive error development in the two eyes; in addition, drug effects and clinical conditions such as anisometropic and astigmatism are also discussed. However, unlike Hung and Ciuffreda's model (1999), which was quantitatively simulated, Wick's model was only descriptive.

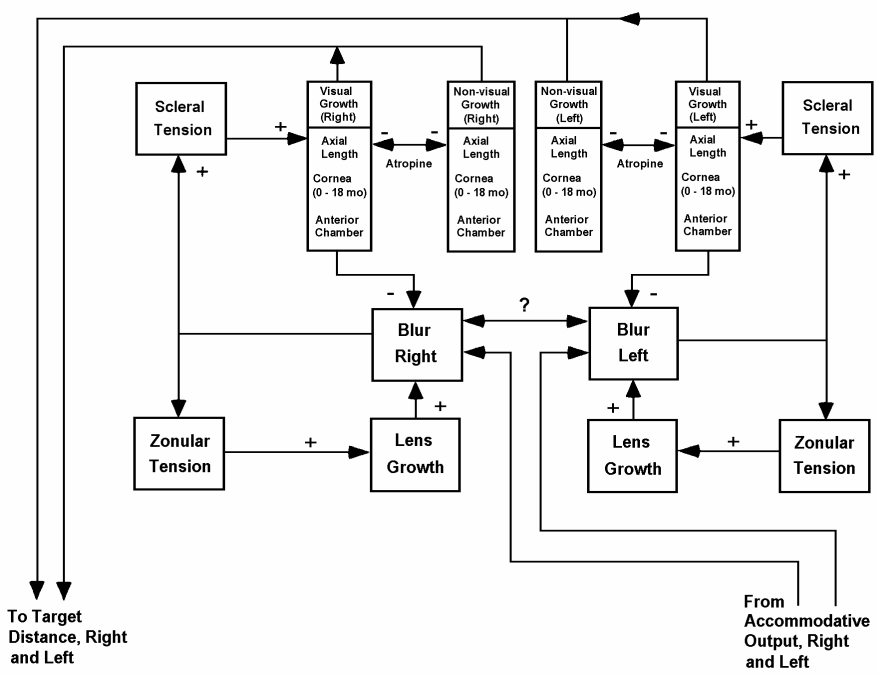

Figure18.6. Wick's (2000) conceptual model of emmetropization takes the form of dual intersecting feedback loops where genetically programmed ocular growth of each eye is altered by blur derived from interactions between accommodation and vergence. The potential influence of suppression on the response of the refractive state to blur is indicated by the crosslink between the blur mechanisms. In the visual growth mechanism, continued relative hyperopic blur (e.g., lag of accommodation at near) increases scleral tension and promotes axial elongation; lens growth is retarded by concurrent reduction in zonular tension. The resulting reduction in lens thickness (with increasing power) and increased axial length decrease the accommodative demand associated with near visual tasks. Visual growth feeds into and combines with genetically programmed ocular growth to result in the final refractive state." Reprinted from Wick (2000), pg. 49, Fig. 1, with permission of J. Optom. Vis. Devel.

Moreover, there are two problems with Wick's conceptual model. First, blur is derived from the combination of accommodative response, axial length, and lens growth, but not from the accommodative stimulus (see Fig. 18.6). Since retinal-image defocus is the difference between the accommodative stimulus and response, it is unclear how the blur signal could be appropriately obtained in the model. Second, his concept that increased scleral tension promotes axial length growth contradicts the findings of reduced scleral rigidity (Castrén and Pohjola, 1961a,b) and decreased tensile strength (Avetisov et al, 1984) in myopic individuals. In addition, instead of

being the driving force for axial elongation, scleral tension is the consequence of active remodeling of the sclera during emmetropization (Reeder and McBrien, 1993; Phillips and McBrien, 1995; Siegwart and Norton, 1999). Further, Ong and Ciuffreda (1997) have argued, based on anatomical and biomechanical studies, that pressure on the sclera itself actually decreases during accommodation, and moreover, its effect is relatively small, thus precluding any direct mechanical role of accommodation in the process of axial elongation. These difficulties reduce the usefulness and general applicability of this model.

Each of these models has provided their own important insights into the overall interactive mechanisms in refractive error development. However, none of these models accounted for two important experimental findings. First, the imposition of plus or minus lenses results in a decrease and increase, respectively in the rate of ocular growth in young animals (Schaeffel et al, 1990; Norton, 1999; Siegwart and Norton, 1999; Smith and Hung, 1999). Second, the rate of ocular growth can be regulated even when the optic nerve is severed, thus precluding any accommodative feedback mechanism in the emmetropization process (Troilo et al, 1987; Wildwoet and Pettigrew, 1988). The development of a new theory, called the Incremental Retinal Defocus Theory, have been an attempt to resolve these long-statnding problems (see below).

18.3 INCREMENTAL RETINAL-DEFOCUS THEORY (IRDT)

To explore the underlying mechanism and to account for the apparently mixed experimental findings, a recent theory of refractive error development was formulated by us (Hung & Ciuffreda, 1999, 2000a-c). Two fundamental insights underlie our theory, which is called the Incremental Retinal-Defocus Theory (IRDT). First, local retinal-defocus magnitude is critical in the development of environmentlly-induced refractive error. The perceived blur is an even-error signal, which provides magnitude but not direction information regarding retinal defocus. Second, manipulations of the visual environment are effective in producing and/or modulating refractive error development mainly during the ocular growth and maturational period. This demonstrates the importance of a time-dependent element in providing the appropriate directional sense. It can be seen, however, that each insight alone is insufficient to provide a workable bidirectionally-sensitive theory. But, when these two are combined, they provide a coherent framework for a unifying theory of refractive error development. Our theory is based on the concept that the change in magnitude of retinal defocus during an increment of genetically-programmed axial length growth provides the critical

information for directional modulation of growth rate. The term genetically-programmed is used to describe the normally-occurring ocular growth that has been pre-programmed genetically. This should be distinguished from environmentally-induced growth that is due to a change in retinal defocus. Both, however, involve neuromodulator release, with the environmentally-induced component acting to modulate the normal genetically-programmed release rate.

17.3.1 Basic Principles of the Theory

[1] *Neuromodulators Control Sensitivity to Changes in Retinal-Image Contrast*

In contrast to neurotransmitters, such as glutamate, acetylcholine, and GABA, which respond rapidly to retinal stimulation (Dowling, 1996), neuromodulators, such as dopamine, seratonin, and neuropeptides (Stone et al, 1989; Iuvone et al, 1991; Dowling, 1996), act over a longer period, and in addition, may cause changes in the neuronal synapses (Windhorst, 1996). An example of synaptic plasticity in the retina can be seen in the interplexiform cells in the retina (Dowling, 1996). These neurons, which contain dopamine, receive their inputs from the amacrine cells in the inner plexiform layer, and then send their outputs back to the horizontal cells in the outer plexiform layer (Werblin, 1973; Kolb, 1994; 1981; Dowling, 1996). Dopamine serves as a neuromodulator by altering the properties of the horizontal cell membrane and decreasing the flow of current across the membrane (Dowling, 1996; Windhorst, 1996). Moreover, because of the center-surround structure of the retina, the interplexiform neurons respond in a graded manner to local retinal-image contrast (Werblin, 1973; Kolb, 1994; Dowling, 1996).

We have proposed that feedback regulation provided by the interplexiform neurons from the inner to outer plexiform layers acts to maintain a relatively constant sensitivity to retinal-image contrast, and furthermore that interplexiform neuronal activity leads to a corresponding change in the neuromodulators (Hung and Ciuffreda, 2000a-c). Such feedback regulation is useful. It precludes the need for a memory mechanism to register and store previous levels of retinal defocus for the purposes of update and comparison. The release of neuromodulators results in synaptic changes in the horizontal cells (Dowling, 1996; Windhorst, 1996). This in turn alters retinal sensitivity to center-surround input, which helps to shift the steady-state operating level to permit responsivity to transient changes in local retinal-image contrast. Thus, the net rate of release of neuromodulators is <u>not</u> dependent on the absolute level of retinal defocus, but rather on the <u>change</u> in retinal-defocus magnitude. The release of neuromodulators also

causes structural changes in the sclera via modulation of proteoglycan synthesis (Rada et al, 1992; Norton & Rada, 1995), wherein an increase in proteoglycan synthesis rate results in greater structural integrity of the sclera, and in turn, a decrease in axial growth rate relative to normal. Conversely, a decrease in proteoglyccan synthesis rate results in less structural integrity of the sclera, and in turn, an increase in axial growth rate relative to normal (Gottlieb et al, 1990; McBrien et al, 1999; Wilsoet, 1998; Christiansen & Wallman, 1991; Marzani & Wallman, 1997; Siegwart & Norton, 1999).

[2] *The Overall Mechanism for Regulating the Rate of Axial Length Growth*

Genetically-programmed mechanisms determine a baseline rate of neuromodulator release that is associated with normal axial growth rate. Retinal defocus-induced changes in the rate of neuromodulator release are superimposed onto this baseline level to result in changes relative to the normal axial growth rate. The net effect of the local-retinal mechanism, as discussed above, is that the change in retinal-defocus magnitude, and in turn the change in the rate of neuromodulator release, are in opposite directions with respect to the change in the rate of defocus-induced axial growth relative to normal. Thus, during an increment of genetically-programmed ocular growth, a change in retinal-defocus magnitude due to the incremental change in ocular geometry provides the directional information needed to modulate the rates of release of neuromodulators and proteoglycan synthesis, which in turn produce structural changes in the sclera for regulation of ocular growth (Siegwart & Norton, 1999; Wildsoet, 1998). For example, during an increment of genetically-programmed ocular growth (over days), if the retinal-defocus magnitude decreases, the axial growth rate increases. This results in relative myopic growth. On the other hand, if the retinal-defocus magnitude increases, the axial growth rate decreases. Hence, this results in relative hyperopic growth. These resultant axial growth rate changes are consistent with the emmetropization process. See Fig. 18.7 and the next section for details.

18.3.2 Applications of the Theory

This theory was tested under five critical experimental conditions to assess the generality of the proposed underlying mechanism. In addition, a MATLAB/SIMULINK model was constructed to demonstrate quantitatively the direct effect of change in retinal defocus via signal cascade through the retinal layers on scleral growth rate.

Lenses

During ocular development, the eye exhibits continuous genetically-programmed growth (Hung and Ciuffreda, 1999, 2000a-c). The imposition of a lens causes changes in retinal defocus, which acts to modulate the genetically-predetermined normal growth rate, and thereby alter overall axial length growth rate. This modulation can be illustrated by the following example. Consider the effect of introducing spherical lenses in front of the eye. The change in size of the blur circle during a small increment of normal genetically-programmed ocular growth for large imposed zero, minus, and plus lenses is shown schematically in Figs. 18.7a, b, and c, respectively. A neuromodulator, such as dopamine, maintains a certain level of neuronal activity related to retinal-image contrast by means of the local retinal feedback mechanism described earlier. The net effect is that the rate of neuromodulator release is dependent not on the absolute level of retinal-defocus magnitude, but rather on the change in retinal-defocus magnitude during the increment of genetically-programmed ocular growth, as was also mentioned earlier. For example, for a zero power lens, there is no change in the size of the blur circle. Thus, no additional neuromodulator is released,

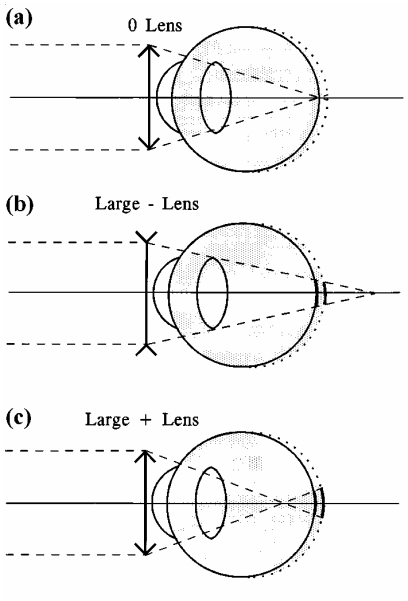

Figure 18.7. Below local blur threshold;
Normal rate of neuromodulators;
Normal growth rate.
Dashed lines represent distant light rays.
Dotted curves represent growth increments.

Decrease in local blur magnitude;
Decrease in rate of neurotransmitters;
Decrease in rate of proteoglycan synthesis
Increase in axial growth rate relative to normal.

Increase in local blur magnitude;
Increase in rate of neuromodulators;
Increase in rate of proteoglycan synthesis;
Decrease in axial growth rate relative to normal.

Reprinted from Hung and Ciuffreda (2000c), pg. 1094, Fig. 1,
with permission of Bull. Math. Biol.

and the normal genetically-based incremental axial growth pattern of the young eye is maintained. With the introduction of a minus lens, however, the size of the blur circle is decreased during the growth increment; thus, the rates of neuromodulator release and in turn proteoglycan synthesis are decreased, thereby resulting in an increase in axial growth rate (Norton, 1999). On the other hand, with the introduction of a plus lens, the size of the blur circle is increased during the growth increment; thus, the rates of neuromodulator release and in turn proteoglycan synthesis are increased, thereby resulting in a decrease in axial growth rate (Norton, 1999). Hence, either a decrease or increase in mean retinal-defocus magnitude during an increment of genetically-programmed axial growth is proposed to cause a change in the rate of neuromodulator release, which in turn leads to biochemically-mediated structural changes in the sclera (Siegwart & Norton, 1999; Wildsoet, 1998), that are manifest as appropriate changes in the rate of axial growth and reflect the active emmetropization process.

Graded Diffusers

The IRDT theory can also be applied to recent experimental results on the effect of graded diffusers in monkeys (Smith & Hung, 2000). Although a diffuser can have complex optical effects (Smith & Atchison, 1997), its primary effect is to disperse or scatter the rays of light that are transmitted through the diffuser. This is schematically represented by a cone of light and seen in the figure as two lines representing the boundaries of the cone (Fig. 18.8a-c). The angle is increased for a stronger diffuser to represent its greater dispersional effect (Fig. 18.8c). This results in a very diffuse blur circle on the retina. Since accommodation would be quite imprecise under this condition, for simplicity, the focal point for the central ray of the cone of diffused light is set midway between the two incremental foveal positions along the visual axis. It can be shown that based on the geometrical configuration using ray tracing, for the weak diffuser with small dispersion (Fig. 18.8a), the decrease in retinal-defocus magnitude during the genetically-programmed incremental growth is relatively minor. Thus, the decrease in neuromodulator and proteoglycan synthesis is small, thereby resulting in a relatively small increase in axial growth rate. On the other hand, for the stronger diffusers with stronger dispersions (Figs. 18.8b, c), there is a progressively greater decrease in retinal-defocus magnitude. Therefore, the intermediate diffuser will result in an intermediate increase in axial growth rate, whereas the strong diffuser will result in the largest increase in axial growth rate. These findings are consistent with experimental results in animals (Smith & Hung, 2000).

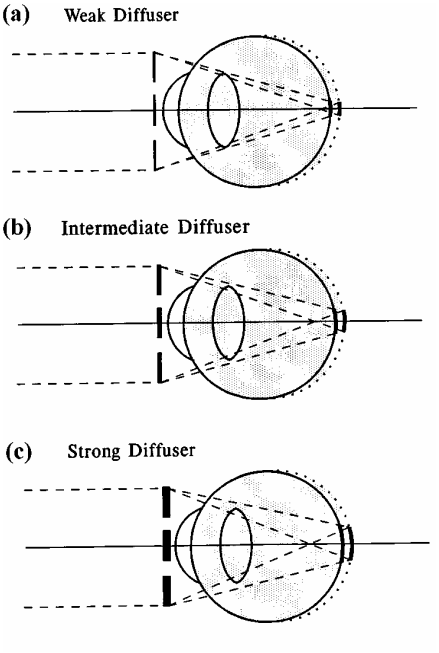

Figure 18.8. Note that the diffuser increases the effective dispersion of any ray of light, resulting in a blur circle. See text for details. Dashed lines represent distant light rays. Dotted curves represent growth increments. See text for details. Reprinted from Hung and Ciuffreda (2000c), pg. 1095, Fig. 2, with permission of Bull. Math. Biol.

Black Occluder

Under the more extreme condition of a full black occluder (Smith & Hung, 2000), there is complete absence of form vision along with a drastically reduced retinal luminance level. Our theory predicts that as a result of the absence of retinal signal-induced feedback regulation of horizontal cells in the dark (Dowling, 1996), there would likewise be a drastic reduction in the rate of neuromodulators, and in turn a substantial decrease in the rate of proteoglycan synthesis (Fig. 18.9a). This will result in a marked increase in the axial growth rate and the development of myopia, which is also consistent with experimental results in animals (Tigges et al, 1990; Iuvone et al, 1991).

Very Strong Diffuser or Removal of Crystalline Lens

For the condition of either a very strong diffuser (Fig. 18.9b) or the removal of the crystalline lens (Fig. 18.9c), there is a large initial increase in retinal-image blur magnitude. Our theory predicts that this will cause an initial increase in the rates of neuromodulators and proteoglycan synthesis, which will result in a decrease in the axial growth rate, and therefore relative

hyperopia. However, the large blur magnitude, with its boundary rays being nearly parallel, does not change substantially during subsequent time increments. This lack of change in retinal-defocus magnitude will result in a normal rate of neuromodulator release, and therefore the subsequent axial growth rate will be nearly normal. Thus, the initial hyperopia is retained (Smith & Hung, 2000).

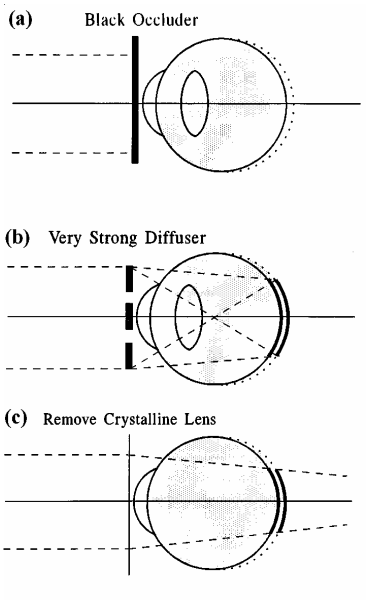

Figure 18.9. (a) Absence of retinal signal-induced feedback regulation in the dark;
Low rate of neuromodulators;
Low rate of proteoglycan synthesis;
High rate of ocular growth.
Dashed lines represent distant light rays.
Dotted curves represent growth increments.

(b & c) Large initial increase in blur magnitude;
Increase in rate of neuromodulators;
Increase in rate of proteoglycan synthesis;
Decrease in axial growth rate relative to normal;
Subsequent growth rate near normal since
change in blur magnitude is relatively small;
Hence, remain hyperopic.

Reprinted from Hung and Ciuffreda (2000c), pg. 1096, Fig. 3,
with permission of Bull. Math. Biol.

Transient Hyperopia

Transient hyperopia following the imposition of a diffuser can be explained as follows (Fig. 18.10). Prior to the imposition of the diffuser, the retinal-defocus magnitude is near or below the threshold level. Thus, there is a relatively small amount of retinal defocus-induced neuromodulator release and proteoglycan synthesis, and the growth rate is determined primarily by genetic factors. However, the sudden imposition of the diffuser results in an immediate increase in retinal-defocus magnitude. Thus, there is a transient increase in the rates of neuromodulators and proteoglycan synthesis. This results in a decrease in axial growth rate, or a transient relative hyperopia. However, subsequently, as the genetically-programmed growth continues, the condition becomes similar to that shown in Figs. 18.8a-c. Since the

boundaries of the light bundles from the diffuser converge beyond the retina, there will now be an incremental decrease in retinal-defocus magnitude. The resultant decrease in the rates of neuromodulators and proteoglycan synthesis, and in turn an increase in axial growth rate, will first effectively null out the initial hyperopia and then eventually develop into myopia (see Figs. 18.8a-c). This can account for the transient nature of the initial hyperopia seen in some of the recent monkey experimental results (Smith & Hung, 2000).

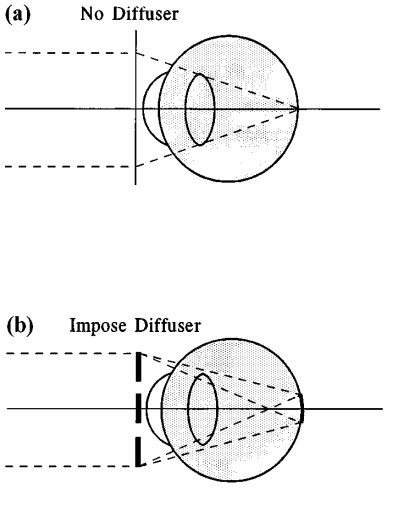

Figure 18.10. Prior to imposition of diffuser, below local blur threshold;

Normal rate of neuromodulators;

Normal rate of proteoglycan synthesis;

Normal growth rate.

Dashed lines represent distant light rays.

Imposition of diffuser results in sudden increase in local blur magnitude;

Thus, there is a transient increase in rate of neuromodulators;

Increase in rate of proteoglycan synthesis;

Decrease in axial growth rate relative to normal;

Resulting in an initial hyperopia;

Subsequent myopic effect during incremental growth first overcomes the initial hyperopia, and then develops into relative myopia.

Reprinted from Hung and Ciuffreda (2000c), pg. 1097, Fig. 4, with permission of Bull. Math. Biol.

The initial transient increase in retinal-defocus magnitude may also explain some recent findings of a greater effect of plus over minus lenses in controlling ocular growth. For example, Wildsoet and Collins (2000) found that imposition of plus/minus multifocal lenses in chicks resulted in a preference towards hyperopic ocular development, which indicates a preference of the plus over the minus lens. Also, Winauer et al (2000) found that chicks compensated to imposed plus lenses even when blurred with diffusers, thus suggesting a particular potency of myopic blur in changing ocular growth rate. These results can be explained by the fact that the imposition of either a plus or a minus lens will cause an initial transient increase in retinal-defocus magnitude. During a subsequent increment of genetically-programmed growth, the plus lens will cause an increase in retinal-defocus magnitude (see Fig. 18.7c), which augments the initial transient increase. On the other hand, the minus lens will cause a decrease in retinal-defocus magnitude (see Fig. 18.7b), which opposes the initial transient increase. The net result is a greater effect of plus over minus lenses during the initial phases of ocular development following such optical manipulations.

Prolonged Nearwork

Finally, the theory can be analyzed for the condition of prolonged nearwork, as in the case of the development of school myopia, wherein relatively small amounts of retinal defocus are present over extended periods of time (i.e., weeks or months) (Ong & Ciuffreda, 1995, 1997). This can be understood in terms of the interactions between two clinical measures: the dynamic nearwork-induced transient myopia (NITM) and the static normal accommodative stimulus/response (AS/R) function (Ciuffreda, 1991, 1998; Ciuffreda & Kenyon, 1983; Ong et al, 1993; Hung, 1998) (Fig. 18.11). NITM refers to the transitory myopic refractive shift found in distance viewing immediately following sustained nearwork (Ong and Ciuffreda, 1995, 1997). It is measured as the difference between post- (Y in Fig. 18.11) and pre-task (■ in Fig. 18.11) accommodative levels at distance. The AS/R function is a static s-shaped curve which shows a slight over-accommodation at distance and progressive under-accommodation at near with increased dioptric demand (Ciuffreda, 1991, 1998).

During nearwork, the accommodative response (AR) lags the accommodative stimulus (AS) (Fig. 18.11, point A; Fig. 18.12a). However, immediately following the nearwork and returning to the far-target viewing, AR exceeds AS more than usual due to the presence of NITM and its relatively slow decay back to the initial pre-task distance refractive state (Figs. 18.11 and 18.12b). This transient myopia can be conceptually regarded as an equivalent low-powered plus lens that is placed in front of the

eye (Fig. 18.12c). The transient myopia remains for a period of time [30 sec or longer (Ong and Ciuffreda, 1995, 1997)]. In returning to nearwork within this slow decay period, the accommodative stimulus is now the net result of the negative optical power due to the distance of the target minus the small equivalent plus lens associated with the residual transient myopia, i.e., the non-decayed portion of the NITM. Thus, the net accommodative stimulus is slightly less (~ 0.25 D) than 4D (point B in Fig. 18.11) (Ong and Ciuffreda, 1997). The response to this reduced effective AS is a slightly reduced AR, and thereby a smaller AE is present. Therefore, the cumulative effect of such repeated, non-fully decayed NITM, which results in repeated transient decreases in retinal defocus at near, is conceptually similar to that of an imposed large static minus lens during an increment of genetically-determined ocular growth (Fig. 18.7b). By the earlier arguments, this results in a decrease in the net rate of release of neuromodulators, a decrease in proteoglycan synthesis, and in turn an increase in the rate of axial growth relative to normal, or relative myopic growth. It is somewhat ironic that rather than representing a failure of the emmetropization process, myopia development is actually a result of the emmetropization process that operates under the constraints of the AS/R function during increments of genetically-programmed ocular growth.

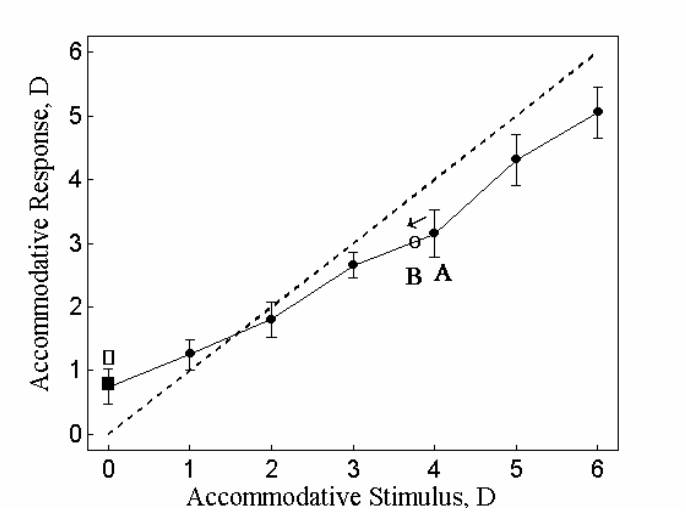

Figure 18.11. Plot of mean accommodative stimulus-response data for 10 visually-normal subjects. Symbols: ● = group mean accommodative response, error bars = ±SEM, ■ = initial pre-task refractive state at distance, Y = initial post-task NITM, data point at A = initial near response, and O = subsequent near response with superimposed non-decayed NITM. Adapted from Ong et al (1993), pg. 199, Fig. 6, with permission from Invest. Ophthal. Vis. Sci.

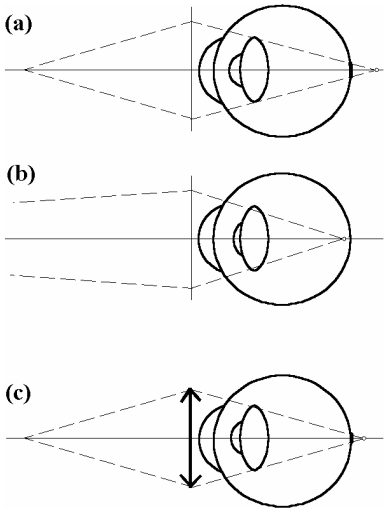

Figure 18.12. Nearwork results in lag of AR and associated hyperopic defocus (pt. A in AS/R curve in Fig. 18.11). Dashed lines represent light rays from object.

Subsequent viewing at far results in a small nearwork-induced transient myopia (NITM).

Plus lens represents equivalent amount of residual transient myopia. Far-to-near carry-over of NITM due to slow decay of crystalline lens power can be represented by an equivalent plus lens. Thus, when returning to nearwork, the effective AS is reduced slightly, and AR is also reduced (i.e., moved down from A to B in the AS/R curve in Fig. 18.11), resulting in a slight decrease in AE, or retinal defocus.

Adapted from Hung and Ciuffreda (2000c), pg. 1099, Fig. 5, with permission of Bull. Math. Biol.

The analysis above also explains why the increase in axial growth rate is primarily associated with prolonged nearwork rather than farwork. This results from a difference in their operating regions on the AS/R curve. It was noted that the net result of repeated NITM is a decrease in the accommodative stimulus, or a shift of AS to the left on the AS/R curve. For nearwork (AS = 4 D), this results in a decrease in retinal defocus magnitude. On the other hand, for farwork (AS $\leq$ 1.5 D), this results in an increase in retinal defocus magnitude. Thus, in contrast to the effect of nearwork discussed above, farwork is analogous to the imposition of a plus lens (see Fig. 18.7c), which according to IRDT, results in a relative decrease in axial growth rate. Furthermore, some individuals (hyperopes and emmetropes) may not develop myopia subsequent to nearwork, because they may have higher sensory blur thresholds for inducing axial length growth than the myopes (Hung & Ciuffreda, 1999; Flitcroft, 2000).

In addition, according to this theory, the rate of ocular growth is dependent on the change in retinal-defocus magnitude regardless of how it is generated. Therefore, in the absence of an increment of genetically-programmed ocular growth, retinal defocus-induced axial elongation due to

prolonged nearwork can still occur as long as the individual exhibits susceptibility to the neurochemical influences on scleral growth. This may explain the finding of form deprived myopia in adolescent animals even after they are past the rapid juvenile growth phase (Troilo et al, 2000b), as well as the finding of axial-based permanent myopia in newly-trained adult microscopists (Adams and McBrien, 1992).

18.3.3 Basic Retinal Anatomy and Physiology of IRDT

Since the IRDT involves detailed aspects of retinal signal processing, a brief review of retinal neural signal transmission is provided below. Signals are transmitted in the retina through three types of neurons: photoreceptors, bipolar cells, and ganglion cells. The photoreceptors (rods and cones) are stimulated by light and relay their signals through bipolar cells, which in turn relay the information through the ganglion cells. The axons of the ganglion cells in the retina form the optic nerve, which transmits retinal-image information to the higher cortical centers. Bipolar cells also receive light stimulus information from neighboring, or surround, photoreceptors via lateral connections from horizontal cells in the outer plexiform layer. This center-surround organizational structure provides local retinal-image contrast information to the "sustained" ganglion cells, which respond to sustained contrast information. On the other hand, "transient" ganglion cells respond to change in the surround via amacrine cells in the inner plexiform layer. Thus, these neurons relay information regarding any change in retinal-defocus magnitude. In addition, interplexiform neurons from the inner-to-outer plexiform layer modulate the long-term sensitivity of horizontal cells to surround input. Thus, this feedback mechanism serves to adjust the steady-state sensitivity level to provide relatively constant sensitivity to changes in local contrast (Dowling, 1996).

18.4 QUANTITATIVE MATLAB/SIMULINK MODEL

A conceptual block diagram of the model is shown in Fig. 18.13a. It is based on the principle that the magnitude of retinal defocus can be represented by the difference in center and surround excitation. A change in this signal, and thus a change in retinal-defocus magnitude, provides the requisite sign for modulating ocular growth. The sensitivity to local retinal-image contrast is maintained at a relatively constant level by means of feedback regulation of horizontal cell gain provided by the interplexiform neurons. This precludes the need for a "memory mechanism" (Norton, 1999) for storing information regarding the immediately previous level of

retinal-defocus magnitude, so that its change can be discerned. The release of neuromodulator in turn results in changes in the rate of scleral proteoglycan synthesis, which causes a change in scleral growth rate. This relative growth rate is added to the ongoing and normal genetically-programmed ocular growth rate to provide the overall axial length growth.

The detailed model is shown in Fig. 18.13b. The sustained pathway consists of the photoreceptor, bipolar, and sustained ganglion cells. It is modulated by surround signals via horizontal cells in the outer plexiform layer to provide local steady-state or sustained contrast information. The transient pathway also consists of photoreceptor, bipolar, and transient ganglion cells. However, it is modulated by surround signals via amacrine cells in the inner plexiform layer to provide information regarding local change or transients in contrast information. Feedback regulation is provided locally by the interplexiform neurons that receive signals for neuromodulator release in the inner plexiform layer and modulate the gain of horizontal cells in the outer plexiform layer to maintain a relatively constant sensitivity to change in local contrast. The center bipolar cell receives a signal derived from the difference between center and summed surround inputs, which represents the summated amount of retinal-image defocus across the overlapping, spatially-contiguous center and surround receptive field area. This signal is differentiated by neural circuitry in the inner plexiform layer, which most likely contains amacrine cells. This change is rectified, so that the "envelope" of the signal, which represents the overall change in retinal-defocus magnitude, drives the rate of neuromodulator release. The neuromodulator, or a cascade of neurochemicals related to the release of the neuromodulator (Wallman, 1997), passes through the choroid to reach the sclera. The transit of the neuromodulator through the choroid may result, at least in the monkey, in a volume change that is observed as a change in choroidal thickness (Curtin, 1985; Cheng et al, 1992; Wildsoet and Wallman, 1995; Marzani and Wallman, 1997; Hung et al, 2000b,c; Troilo et al, 2000a*)*. This may explain why, as expected, choroidal thickness changes in the monkey are correlated with changes in retinal-defocus magnitude, but the optical change associated the thickness change is too small to account for any significant contribution towards full emmetropization (Hung et al, 2000b.c; Troilo et al, 2000a). On the other hand, the neuromodulator that reaches the sclera modifies proteoglycan synthesis to result in changes in ocular growth that does provide nearly full emmetropization, as described in the schematic model (Fig. 18.13a).

Model simulation responses to center and surround stimuli are shown in Figs. 18.14 a-d. The center stimulus representing sharp focus consists of a ± 1 amplitude (in arbitrary units representing change in luminance relative to the background level) peak-to-peak, 0.1 Hz, square-wave signal. The surround stimuli, representing varying degrees of retinal-image defocus,

consists of the same square wave but modulated by different step levels over the time span of the simulation. Fig. 18.14a shows the various steps of modulation of the surround amplitude (solid) and the feedback-regulated change in gain of the horizontal cells. As noted above, this provides relatively constant sensitivity to changes in retinal-defocus magnitude. The pulse-like responses for the rates of neuromodulator release (solid) and proteoglycan synthesis (dashed) are shown in Fig. 18.14b. The change in proteoglycan synthesis rate in turn causes changes in the scleral growth rate relative to normal (Fig. 18.14c). Finally, the cumulative change in axial length relative to normal is shown in Fig. 18.14d. These results clearly demonstrate that the model is able to simulate the bi-directional aspects of choroidal and scleral axial length changes found experimentally.

Figure 18.13. (See next page). (a) Conceptual block diagram model of the retinal-defocus pathway for regulating sclera growth. The difference between center and surround excitation provides the retinal-defocus signal. The derivative of the signal drives the release of neuromodulators, which provides the feedback via interplexiform neurons to regulate horizontal cell gain. In addition, release of neuromodulators causes changes in the rate of proteoglycan synthesis, and in turn relative scleral growth rate. (b) Detail block diagram model depicting the regulation of scleral growth rate. The retinal layers (outer to inner) are arranged from left to right: photoreceptor, outer plexiform, bipolar, inner plexiform, and ganglion. The sustained pathway consists of center photoreceptor, center bipolar B, and sustained ganglion cell. Horizontal cell, whose gain is regulated by feedback via interplexiform cells, relays surround information to modify sustained ganglion output. The transient pathway consists of center photoreceptor, center bipolar A, and transient ganglion cell. Amacrine cell relay change in surround information to modify transient ganglion output. Center bipolar B signal consists of retinal-defocus information and passes through a rectifier, lowpass filters, and elements representing neuromodulator release, the choroid, and proteoglycan synthesis. This is inverted to provide relative scleral growth rate relative to normal. Adapted from Hung and Ciuffreda (2000c), pg. 1101, Figs. 6a,b, with permission of Bull. Math. Biol.

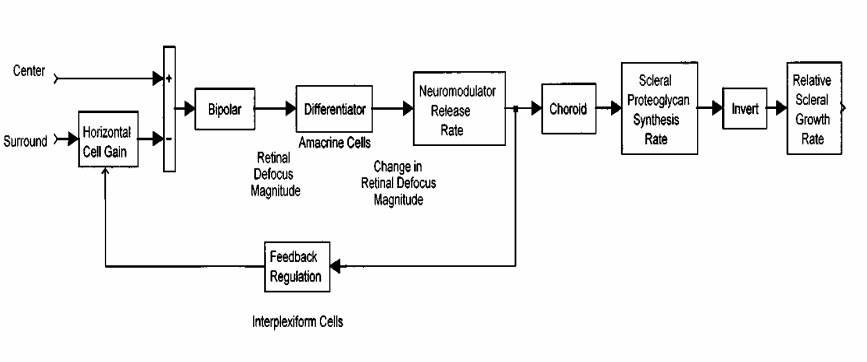

Fig. 18.13a.

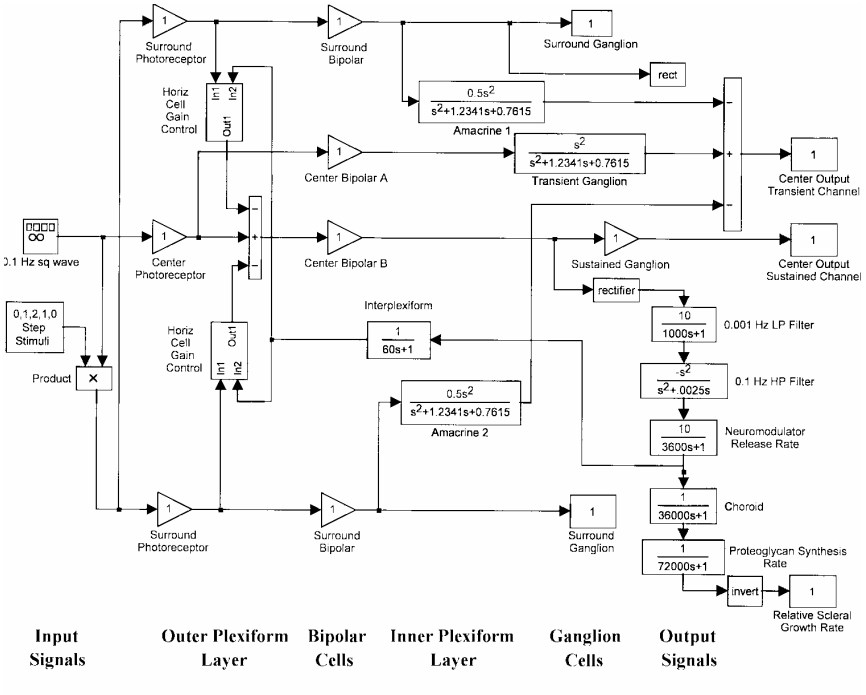

Fig. 18.13b.

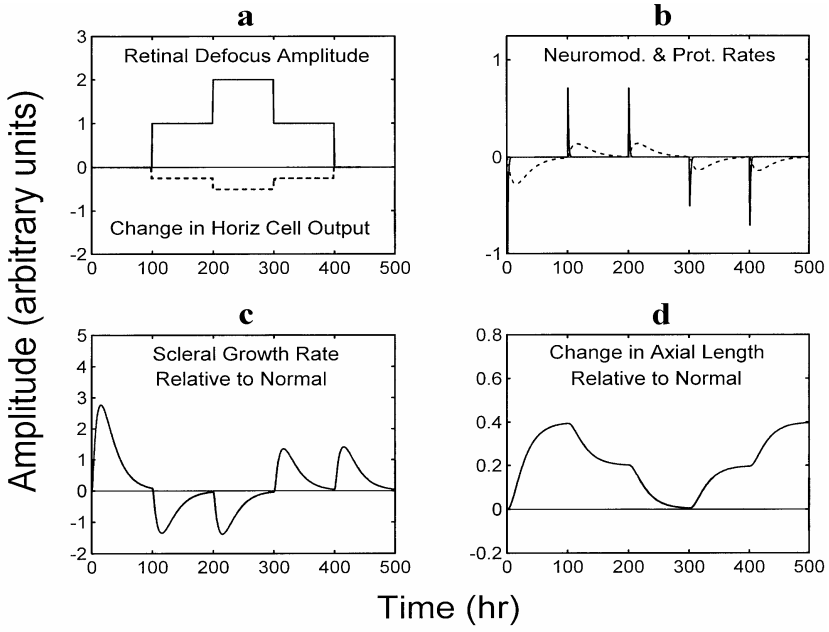

Figure 18.14. (a) Envelope of surround stimulus representing various levels of defocus (solid). Changes in horizontal cell output, which are regulated by interplexiform neuronal feedback, shows a complementary response to surround defocus (dashed). (b) Pulses of rates of neuromodulator release (solid) and proteoglycan synthesis (dashed) occur at the transitions of surround stimulus (see Fig. 18.14a). (c) Rate of scleral growth relative to normal follows the pulses in the rate of proteoglycan synthesis (see Fig. 18.14b). (d) Integration of scleral growth rate provides the change in axial length relative to normal. The direction of change is consistent with experimental findings and with the analysis provided by the schematic model. Adapted from Hung and Ciuffreda (2000c), pg. 1103, Fig. 7, with permission of Bull. Math. Biol.

18.5 SUMMARY AND CONCLUSIONS

Emmetropization appears to be governed by a relatively simple mechanism, which has been described by our newly proposed Incremental Retinal-Defocus Theory (Hung and Ciuffreda, 1999, 2000). The theory states that the rate of change of retinal defocus determines the rate of release of neuromodulators, which modulates rate of proteoglycan synthesis, and in turn regulates the rate of scleral growth. Schematic analysis of the theory has

provided a clear explanation for the eye's ability to grow in the appropriate direction under a wide range of experimental conditions including lens, diffusers, black occluder, and removal of the crystalline lens. In addition, the theory has been able to explain how prolonged nearwork could lead to increased cumulative decrease in proteoglycan synthesis, and thereby increased axial growth and permanent myopia. The critical point is that the detection mechanism does not depend on the sign of the blur, but rather on the change in blur magnitude that is either environmentally-induced or results from an increment of genetically-programmed ocular growth. And, it is not necessary to invoke more complicated processes, such as sensing and analyzing of chromatic aberration, spherical aberration, spatial gradient of blur, or spatial frequency content (Ciuffreda, 1991, 1998). Thus, this unifying theory provides an understanding of the basic underlying retinal mechanism for detecting blur magnitude, and furthermore explains how the neurochemical signal is processed to modulate the rate of eye growth, and in turn the resultant development of axial myopia.

18.6 REFERENCES

Adams, D. W., and McBrien, N. A. 1992, Prevalence of myopia and myopic progression in a population of clinical microscopists, *Optom. Vis. Sci*. **69**: 467-473.

Alward, W.L., Bender, T.R., Demske, J.A., and Hall, D.B., 1985, High prevalence of myopia among young adult Yupik Eskimo, *Can. J. Ophthalmol*. **20**: 241-245.

Avetisov, E. S., Savitskaya, N. F., Vinetskaya, M. I., and Iomdina, E. N., 1984, A study of biochemical and biomechanical qualities of normal and myopic eye sclera in humans of different age groups, *Metab. Pediatr. Syst. Ophthalmol*. **7**: 183-188.

Bartmann, M., and Schaeffel, F., 1994, A simple mechanism for emmetropization without cues from accommodation or colour, *Vis. Res*. **34**: 873-876.

Bennett, A. G., and Rabbetts, R.B., 1989, *Clinical Visual Optics*, Butterworth-Heinemann, Woburn, MA, pg. 75.

Blackie, C. A. and, Howland, H. C., 1999, Extension of the Flitcroft model of emmetropization: inclusion of pupil size, *Ophthal. Physiol. Opt.* **19**: 112-125.

Bradley, D. V., Fernandes, A., Tigges, M., and Boothe, R.G., 1996, Diffuser contact lenses retard axial elongation in infant rhesus monkeys, *Vis. Res*. **36**: 509-514.

Castrén, J. A., and Pohjola, S., 1961a, Refraction and scleral rigidity, *Acta Ophthalmol*. **39**: 1011-1014.

Castrén, J. A., and Pohjola, S., 1961b, Scleral rigidity in puberty, *Acta Ophthalmol*. **39**: 1015-1019.

Cheng, H.-M., Omah, S. S., and Kwong, K. K., 1992, Shape of the myopic eye as seen with high-resolution magnetic resonance imaging, *Optom. Vis. Sci*. **69**: 698-701.

Christiansen, A. M. and Wallman, J., 1991, Evidence that increased scleral growth underlies visual deprivation myopia in chicks, *Invest. Ophthal. Vis. Sci*., **32**: 2134-2150.

Ciuffreda, K. J., 1991, Accommodation and its anomalies, in: *Vision and Visual Dysfunction*: *Visual Optics and Instrumentation*, Vol. 1, W. N. Charman, ed., Macmillan, London, pp. 231-279.

Ciuffreda, K. J., 1998, Accommodation, pupil, and presbyopia, in: *Borish's Clinical Refraction,* W. J. Benjamin, ed, , W. B. Saunders Co, Philadelphia, PA, pp. 77-120.

Ciuffreda, K. J., Kenyon R. V., 1983, Accommodative vergence and accommodation in normals, amblyopes, and strabismics, in: *Vergence Eye Movements: Basic and Clinical Aspects,* C. M. Schor and K. J. Ciuffreda, eds., Butterworths, Boston, MA, pp. 101-173.

Ciuffreda, K. J., and Wallis, D. M., 1998, Myopes show increased susceptibility to nearwork aftereffects, *Invest. Ophthal. Vis. Sci*. **39**: 1797-1803.

Curtin, B. J., 1985, The etiology of myopia, in: *The Myopias: Basic Science and Clinical Management*, Harper & Row, Philadel. PA, pp. 61-151.

Dowling, J. E., 1996, Retinal processing of vision, in *Comprehensive Human Physiology: From Cellular Mechanisms to Integration*, *Vol. 1,* Greger R and U. Windhorst, eds., Springer-Verlag, Berlin, pp. 773-778.

Fledelius, H. C., and Stubgaard, M., 1986, Changes in refraction and corneal curvature during growth and adult life. A cross-sectional study, *Acta Ophthalmol*. **64**: 487-491.

Flitcroft, D. I., 1998, A model of the contribution of oculomotor and optical factors to emmetropization and myopia, *Vis. Res*., **38**: 2869-2879.

Goh, W.S., and Lam, C.S., 1994, Changes in refractive trends and optical components of Hong Kong Chinese aged 19-39, *Ophthal. Physiol. Opt*. **14**: 378-382.

Goldschmidt, E., 1968, On the etiology of myopia - an epidemiological study. *Acta Ophthalmol.* **98 (suppl)**: 1-72.

Goss, D. A., and Erickson, P., 1987, Meridional corneal components of myopia progression in young adults and children, *Am. J. Optom. Physiol. Opt.* **64**: 475-481.

Goss, D. A., Hampton, M. J., and Wickham, M. G., 1988, Selected review on genetic factors in myopia, *J. Am. Optom. Assoc*. **59**: 875-884.

Goss, D. A., and Jackson, T. W., 1993, Cross-sectional study of changes in the ocular components in school children, *Appl. Opt*. **32**: 4169-4173.

Goss, D. A., and Wickham, M. G., 1995, Retinal-image mediated ocular growth as a mechanism for juvenile onset myopia and for emmetropization, *Doc. Ophthalmol*. **90**: 341-375.

Goss, D. A., and Winkler, R. L., 1983, Progression of myopia in youth: age of cessation, *Am. J. Optom. Physiol. Opt*. **60**: 651-658.

Gottlieb, M. D., Joshi, H. B., and Nickla, D. L., 1990, Scleral changes in chicks with form-deprived myopia, *Curr. Eye Res*. **9**: 1157-1165.

Grosvenor, T., and Goss, D. A., 1998, Role of the cornea in emmetropia and myopia, *Optom. Vis. Sci*. **75**: 132-145.

Grosvenor, T., and Goss, D. A., 1999, *Clinical Management of Myopia*. Butterworth-Heinemann, Boston, MA, pp. 49-62.

Gwiazda, J., Thorn F., Bauer J., and Held, R., 1993, Emmetropization and the progression of manifest refraction in children followed from infancy to puberty, *Clin. Vis. Sci.* **8**: 337-344.

Hosaka, A., 1988, Population studies - myopia experience in Japan, *Acta Ophthalmol (Supp) (Kbh).* **185**: 37-40.

Hung, G. K., 1990, Fixation disparity under open- and closed-loop accommodation, *Ophthal. Physiol. Opt*. **10**: 211-214.

Hung, G. K., 1992. Adaptation model of accommodation and vergence, *Ophthal. Physiol. Opt*. **12**: 319-326.

Hung, G. K., 1998, Sensitivity analysis of the stimulus-response function of a static nonlinear accommodation model, *IEEE Trans Biomed Engin*. **45**: 335-341.

Hung, G. K., and Ciuffreda, K. J., 1999, Model of refractive error development, *Cur. Eye. Res*., **19**: 41-52.

Hung, G. K. and Ciuffreda, K. J., 2000a, Differential retinal-defocus magnitude during eye growth provides the appropriate direction signal, *Med. Sci. Monitor*. **6**: 791-795.

Hung, G. K., and Ciuffreda, K. J., 2000b, Quantitative analysis of the effect of near lens addition on accommodation and myopigenesis, *Cur. Eye. Res*. **20**: 293-312.

Hung, G. K., and Ciuffreda, K. J., 2000c, A unifying theory of refractive error development, *Bull. Math. Biol*. **62**: 1087-1108.

Iuvone, P. M., Tigges, M., Stone, R. A., Lambert, S., and Laties, A. M., 1991, Effect of apomorphine, a dopamine receptor agonist, on ocular refraction and axial elongation in primate model of myopia, *Invest. Ophthal. Vis. Sci*. **32**: 1674-1677.

Javitt, J. C., and Chiang, Y. P., 1994, The socioeconomic aspects of laser refractive surgery, *Arch. Ophthalmol*. **112**: 1526-1530.

Jiang, B. C. and Woessner, W. M., 1996, Increase in axial length is responsible for late-onset myopia, *Optom. Vis. Sci*. **73**: 231-234.

Kolb, H., 1994, The architecture of functional neural circuits in the vertebrate retina. The Proctor Lecture, *Invest. Ophthalmol. Vis. Sci.* **35**: 2385-2404.

Lam, C. S., Goh, W. S., Tang, Y. K., Tsui, K. K., Wong W. C., and Man, T. C., 1994, Changes in refractive trends and optical components of Hong Kong Chinese aged over 40 years, *Ophthal. Physiol. Opt*. **14**: 383-388.

Lin, L. L. K., Shih, Y. F., Lee, Y. C., Hung, P. T., and Hou, P. K., 1996, Changes in ocular refraction and its components among medical students - a 5-year longitudinal study, *Optom. Vis. Sci*. **73**: 495-498.

Kimura, T. 1965, Developmental change of the optical components in twins, *Acta Soc. Ophthalmol. Jpn*. **69**: 963-969.

Mahlman, H. E. 1982, *Handbook of Federal Vision Requirements and Information*. Professional Press, Chicago, IL, USA, pp. 8-18.

Marzani, D., and Wallman, J., 1997, Growth of the two layers of the chick sclera is modulated reciprocally by visual conditions, *Invest. Ophthal. Vis. Sci*. **38**: 1726-1739.

McBrien, N. A., Gentle, A., and Cottriall, C., 1999, Optical correction of induced axial myopia in the tree shrew: implications for emmetropization, *Optom. Vis. Sci*. **76**: 419-427.

McBrien, N. A., and Millodot, M., 1986, The effect of refractive error on the accommodative response gradient, *Ophthal. Physiol. Opt*. **6**: 145-149.

Medina, A., 1987, A model of emmetropization, the effect of corrective lenses, *Acta. Ophthalmol*. **65**: 585-571.

Medina, A., and Fariza, E., 1993, Emmetropization as a first-order feedback system, *Vis. Res*. **33**: 21-26.

Mutti, D.D., Zadnik K., and Adams, A.J., 1996, Myopia. The nature vs nurture debate goes on, *Invest. Ophthal. Vis. Sci*. **37**: 952-957.

Norton, T. T., 1999, Animal models of myopia: learning how vision controls the size of the eye, *Instit. Lab. Animal Res. Journal*. **40**: 59-77.

Norton, T. T., and Rada, J. A., 1995, Reduced extracellular matrix in mammalian sclera with induced myopia, *Vis. Res*. **35**: 1271-1281.

O'Leary, D. J., Chung, K. M., and Mohikin, N., 2000, Undercorrection causes more rapid progression of myopia in children, *Am. Acad. Optom. 2000 (Abstract)*, pg. 24.

O'Leary, D. J., Chung, K. M., and Othman, S., 1992, Contrast reduction without myopia induction in monkey, *Invest. Ophthal. Vis. Sci*. **33**: S712.

Ong, E., and Ciuffreda, K. J., 1995, Nearwork-induced transient myopia - a critical review, *Doc. Ophthalmol*. **91**: 57-85.

Ong, E., and Ciuffreda, K. J., 1997, *Accommodation, Nearwork, and Myopia,* Optometric Extension Program Foundation, Inc, Santa Ana, CA, pp. 76-96, 177-201.

Ong, E. , Ciuffreda, K. J., and Tannen, B., 1993, Static accommodation in congenital nystagmus, *Invest. Ophthal. Vis. Sci*. **34**: 194-204.

Pässinen, O., Hemminki, E., and Klemetti, A., 1989, Effect of spectacle use and accommodation on myopia progression: final results of a three-year randomised clinical trial among schoolchildren, *Br. J. Ophthalmol*. **73**: 547-551.

Phillips, J. R., and McBrien, N. A., 1995, Form deprivation myopia: elastic properties of the sclera. *Ophthal. Physiol. Opt*. **15**: 357-362.

Rada, J. A., McFarland, A. L., Cornuet, P. K., and Hassell, J. R., 1992, Proteoglycan synthesis by scleral chondrocytes is modulated by a vision dependent mechanism, *Cur. Eye Res*. **11**: 767-782.

Reeder, A. P., and McBrien, N. A., 1993, Biochemical changes in the sclera of tree shrew with high degrees of experimental myopia, *Ophthal. Physiol. Opt*. **13**: 105.

Rosenfield, M., and Gilmartin, B., 1998, Myopia and nearwork: causation or merely association?, in: *Myopia and Nearwork*, M. Rosenfield and B. Gilmartin, eds., Butterworth-Heinemann, Oxford, pp. 193-206.

Scammon, R. E., and Armstrong, E. L., 1925, On the growth of the human eyeball and optic nerve, *J. Comp. Neurol*. **38**: 165-219.

Schaeffel, F., and Howland, H. C., 1988, Mathematical model of emmetropization in the chicken, *J. Opt. Soc. Am. A* **5**: 2080-2086.

Siegwart, J. T. Jr., and Norton, T. T., 1999, Regulation of the mechanical properties of tree shrew sclera by the visual environment, *Vis. Res*. **39**: 387-407.

Smith, G., and Atchison, D. A., 1997, *The Eye and Visual Optical Instruments*, Cambridge Univ. Press, Cambridge, United Kingdom, pp. 274, 796.

Smith, E. L., and Hung, L. F., 1999, The role of optical defocus in regulating refractive development in infant monkeys, *Vis. Res*. **39**: 1415-1435.

Smith, E. L., and Hung, L. F., 2000, Form deprivation myopia in monkeys is a graded phenomenon, *Vis. Res*. **40**: 371-381.

Sorsby, A., Sheridan, M., and Leary, G. A., 1962, *Refraction and Its Components in Twins,* London: Her Majesty's Stationary Service.

Sperduto, R. D., Seigel, D., Roberts, J., and Rowland, M., 1983, Prevalence of myopia in the United States, *Arch. Ophthalmol*. **101**: 405-407.

Stark, L., 1968, *Neurological Control Systems, Studies in Bioengineering*, Plenum Press, New York, pp. 205-219.

Stone, R. A., Lin, T., and Laties, A. M., 1989, Retinal dopamine and form-deprivation myopia, *Proc. Natl. Acad. Sci*. **86**: 704-706.

Tigges, M., Tigges, J., Fernendes, A., Effers, H. M., and Gammon, J. A., 1990, Postnatal axial eye elongation in normal and visually deprived rhesus monkeys, *Invest. Ophthal. Vis. Sci.* **31**: 1035-1046.

Troilo, D., 1989, *The Visual Control of Eye Growth in Chicks,* Ph. D. Dissertation, Faculty of Biology, City University of New York, New York, NY.

Troilo, D., Gottlieb, M. D., and Wallman, J., 1987, Visual deprivation causes myopia in chicks with optic nerve section, *Cur. Eye Res*. **6**: 993-999.

Troilo, D., Nickla, D. L., and Wallman, J., 2000a, Choroidal thickness changes during altered eye growth and refractive state in a primate, *Invest. Ophthal. Vis. Sci.* **41**: 1249-1258.

Troilo, D., Nickla, D. L., and Wildsoet, C. F., 2000b, Form deprivation myopia in mature common Marmoset (Callitbrix jaccbus), *Invest. Ophthal. Vis. Sci*. **41**: 2043-2049.

Wallman, J., 1997,. Can myopia be prevented? in: *14th Biennial Research to Prevent Blindness Science Writers Seminar in Ophthalmology*, Research to Prevent Blindness, New York, pp. 50-52.

Werblin, F., 1973, Control of sensitivity of the retina, *Sci. Am*. **228 (1)**: 71-79.

Wick, B., 2000, On the etiology of refractive error - Parts I-III, *J. Optom. Vis. Devel*. **31**: 5-21, 48-63, 93-99.

Wildsoet, C. F., 1998, Structural correlates of myopia, in: *Myopia and Nearwork*, M. Rosenfield and B. Gilmartin, eds., Butterworth-Heinemann, Oxford, pp. 32-51.

Wildsoet, C. F., and Collins, M. J., 2000, Competing defocus stimuli of opposite sign produce opposite effects in eyes with intact and sectioned optic nerves in the chick, *Invest. Ophthal. Vis. Sci*. **41**: S738.

Wildsoet, C. F., and Pettigrew, J. D., 1988, Experimental myopia and anomalous eye growth patterns unaffected by optic nerve section in chickens: Evidence for local control of eye growth, *Clin. Vis. Sci.* **3**: 99-107.

Wildwoet, C. F., and Wallman, J., 1995, Choroidal and scleral mechanisms of compensation for spectacle lenses in chicks, *Vis. Sci*. **35**: 1175-1194.

Wilson, J. R., Fernandes, A., Chankler, C. V., Tigges, M., Boothe, R. G., and Gammon, J. A., 1987, Abnormal development of the axial length of aphakic monkey eyes, *Invest. Ophthal. Vis. Sci*. **28**: 2096-2099.

Winauer, J. A., Zhu, X., Park, T., and Wallman, J., 2000, Is myopic blur more important than sharp vision for positive-lens compensation? *Invest. Ophthal. Vis. Sci*. **41**: S136.

Windhorst, U., 1996, Specific networks of the cerebral cortex: functional organization and plasticity, in: *Comprehensive Human Physiology: From Cellular Mechanisms to Integration. Vol. 1*, R. Greger and U. Windhorst, eds., Springer-Verlag, Berlin, pp. 1105-1136.

Woodruff, M.E., and Samek M.J., 1977, A study of the prevalence of spherical equivalent refractive states and anisometropia in Amerind population in Ontario, *Can. J. Public Health*. **68**: 414-424.

Wu, M. M.-M., and Edwards, M. H., 1999, The effect of having myopic parents: An analysis of myopia in three generations, *Optom. Vis. Sci.* **76**: 387-392.

Yackle, K., and Fitzgerald, D. E., 1999, Emmetropization: an overview, *J. Behav. Optom*. **10**: 38-43.

Young, F.A., Leary, G.A., Baldwin, W.R., West, D.C., Box, R.A., Harris, E., and Johnson, C., 1969, The transmission of refractive errors within eskimo families, *Am. J. Optom. Arch. Am. Acad. Optom*. **46**: 676-685.

Zhang, M.-Z., Saw, S.-M., Hong, R.-Z., Fu, Z.-F., Yang, H., Shui, Y.-B., Yap, M. K. H., and Chew, S.-J., 2000, Refractive errors in Singapore and Xiamen, China - A comparative study in school children aged 6 to 7 years, *Optom. Vis. Sci.,* **77**: 302-308.